V European Conference on Computational Fluid Dynamics
ECCOMAS CFD 2010
J. C. F. Pereira and A. Sequeira (Eds)
Lisbon, Portugal,14-17 June 2010

A MULTI-FIDELITY FRAMEWORK FOR DESIGNING COMPLIANT FLAPPING WINGS

D.J. Willis *, and H. Salehipour *

* University of Massachusetts at Lowell,
Department of Mechanical Engineering, One University Ave., Lowell, MA, 01854, USA
e-mail: david_willis@uml.edu, hesam_salehipour@student.uml.edu

Key words: multi-fidelity, flapping, wing design, potential flow

Abstract. *We present a multi-fidelity approach for analyzing and designing morphing wings for flapping wing MAVs. Our focus in this paper is on the two lower fidelity levels in our framework, namely, (1) a wake-only energetics model and (2) an unsteady potential flow, doublet lattice method aerodynamics solver. The wake-only energetics model is used to examine the flapping kinematics design space and determine optimal flapping motions and wake-vorticity distributions at a variety of flight speeds. The thin-membrane wing, potential flow solver is used to inverse design and analyze the wing geometry that produces that particular energetically optimum wake-vorticity-distribution. The resulting capability allows us to robustly traverse lower fidelity methods and rapidly design flapping wings for micro aerial vehicle applications. We present and discuss an example of the multi-fidelity analysis that is similar to a medium sized fruit bat, Cynopterus brachyotis.*

1 INTRODUCTION

The biologically inspired Micro Aerial Vehicle (MAV) design space is large and complex. Simply observing of nature we can hypothesize that flapping frequency, flapping motions, and flapping amplitude as well as wing twist or local incidence will likely all play a vital role in flight performance. While directly mimicking nature is one option for MAV design, a more robust design strategy involves understanding the flapping parameter requirements and dependencies. Computation presents a natural approach for examining and manipulating flapping parameters. Specification of different flapping parameters is a simple task in the computational environment; however, depending on the aerodynamics analysis method, the simulation of a large number of potential designs may be impractical. Similarly, if the computational method lacks too much physical or geometric fidelity, there may be insufficient information to perform large or fine scale improvements to the design. As such, a multi-fidelity approach to design space exploration and MAV design evaluation has been proposed [1, 2]. Starting from computationally efficient wake only methods [3, 4], we can evaluate large regions of the design space. As we narrow in on specific design parameters, higher fidelity representations are used to verify the design philosophy and drive changes to the design.

In this paper we describe briefly the multi-fidelity framework that we use for analyzing and designing flapping winged vehicles and animals; however, our main focus is on the newly refined transition from low-fidelity wake-only representations of a flying vehicle to a first geometric representation of that flapping wing. This paper describes the steps that allow us to seamlessly transition between wake-only analysis results and actual flapping wing geometries. As we will show, the method is effective for determining wing shapes given a target wake circulation distribution and a wing planform as a starting point.

1.1 Previous Work

Many different approaches for analyzing flapping flight have been proposed. While these approaches display a diversity of physical and geometric fidelity levels, there are only a few examples of robust and consistent multi-fidelity MAV design. Much research work has been devoted to the development of differing geometric and physical fidelity aerodynamics tools for examining flapping flight. Investigations performed with these tools have shown significant promise for simpler problems such as two-dimensional [6, 2] and three-dimensional [6, 1] flapping. Unfortunately, the transition between fidelity levels is occasionally awkward, with new geometric and physical information being introduced into each fidelity refinement in the analysis. For instance, at lower fidelity levels, the wing geometry is represented simply using a lifting line (or wake in our case); whereas, at higher fidelity levels, the full wing geometry and fluid domain must be defined for domain discretization. Each fidelity level has a distinct purpose in the design process; however, a multi-fidelity approach is severely hampered when transitioning between fidelity levels is a challenge.

The multi-fidelity framework that we use [6, 1] incorporates three fundamental levels of modeling, within each multiple tools may exist:

1. **Wake-Only Energetics Modeling** [3, 7, 4, 5]: At the lowest fidelity level, a wake only aerodynamics tool is used to determine the optimal circulation distribution for a given flight condition. This tool has recently been used in the development of an energetics analysis framework that permits rapid design space evaluation [4, 5].

2. **Potential Flow Modeling** [8, 6, 9, 1]: At this fidelity level, a lower-fidelity physical representation of the fluid (irrotational and incompressible) is used. This allows us to rapidly determine the flow velocity and pressure around the flapping wings without significant time investment – however, this prediction comes with limited information about viscous effects. While the panel method approach is lower fidelity, it still captures the unsteady inviscid flow reasonably when the flow remains attached.

3. **Navier-Stokes Simulations** [10, 11]: At the highest fidelity level a Navier-Stokes computational model is used to validate the predictions of lower fidelity explorations. The addition of viscous effects int he physical model greatly increases the computational complexity. At this level of fidelity a high order discontinuous Galerkin solution method is used.

At the early stage of design, rapid evaluation of all possible reasonable candidate designs is desired. We use lower fidelity tools in these situations to determine general flapping parameter choices. Unfortunately, the step changes in fidelity between these lower fidelity levels require the introduction of significant amounts of new information. For example, transitioning between our wake-only models and a three-dimensional thin-wing representation requires the introduction of a complete wing geometry. In this paper, we show a robust method of connecting and interacting at the wake-to-wing representation stage in the flapping wing design process.

While we do not describe the use of the higher fidelity tools in this paper, the extension is relatively simple.

2 DESCRIPTION OF THE MULTI-FIDELITY MODELS

Below we briefly describe the wake-only method and its use in evaluating the flapping design space. Following the discussion of the wake-only energetics method, we describe the tool which we propose for transitioning between a wake-only analysis and a full geometry analysis.

2.1 Low Fidelity Energetics Model

Our energetics model uses a wake-only, optimal circulation analysis as the basis of the aerodynamic computations [3]. The wake-only tool, *HallOpt*, determines the minimum

Velocity (m/s)	3	4	5	6	7	8	9
C_L	2.39	1.35	0.86	0.60	0.44	0.34	0.27
C_T	0.860	0.290	0.120	0.067	0.051	0.044	0.036
Amplitude (deg)	65.3	55.5	51.1	50.8	53.7	58.5	64.2
Frequency (Hz)	9.97	9.57	9.18	8.80	8.43	8.07	7.71

Table 1: The predictions for force coefficients, flapping amplitude and flapping frequency at incremental velocities for *Cynopterus brachyotis*.

power wake circulation distribution for a desired set of flight forces and a specific wake geometry [7]. In our current implementation of the energetics model, the wake geometry is a simple harmonic up-down flapping motion about a center body hinge; however, this does not restrict future investigations of more complex flapping motions. We use this wake-only aerodynamics model as a basis for the preliminary comparison of flight energetics in a design setting.

Using the wake-only model, we construct a large *offline* database of all possible flapping parameters (flapping amplitude and flapping frequency), their associated forces (viscous-inviscid decoupled drag coefficients, lift coefficient, etc.) and their associated energetics (the viscous-inviscid decoupled power) [4, 5]. We construct this *offline* database so that it is Reynolds number independent as well as flapper aspect ratio (geometry) independent. The current *offline* database is comprised of approximately $14,500,000$ individual wake-only computations that can be rapidly accessed. Due to the comprehensive sweep of all reasonable flapping parameters, the offline database is only computed once for a given set of flapping parameters. This database is queried in subsequent portions of the energetics evaluation to provide pre-computed data to those analyses.

Following the construction of the *offline* database, we introduce an *intermediate* computation that constructs $C_L - C_T$ response surfaces for the power coefficient and its components, the force coefficients and flapping parameters of interest [4, 5]. The *intermediate* calculation introduces general flapper dependencies (such as Reynolds number, and wing aspect ratio). These $C_L - C_T$ response surfaces are then used in a rapid evaluation *online* component. In the *online* code, the geometry and weight of the vehicle or animal are inputted and the dimensionality force balance ($L = mg\cos(\theta)$ and $T = D + mg\sin(\theta)$, where θ is the climb angle) is performed. The *online* code predicts the optimal aerodynamics power (and power components) as a function of flight speed as well as the lift, drag, amplitude, and frequency. In addition to the energetics outputs, the wake-only model can be used to predict the wake circulation distributions for different flight velocities. As we show in this paper, these wake-circulation distributions are a particularly useful starting point for designing efficient flapping MAV wings. For *Cynopterus brachyotis*, the plot in figures 1-2 illustrate the components of flight power, flight force coefficient, flapping frequency and flapping amplitude as a function of forward velocity. This information is summarized in table 1.

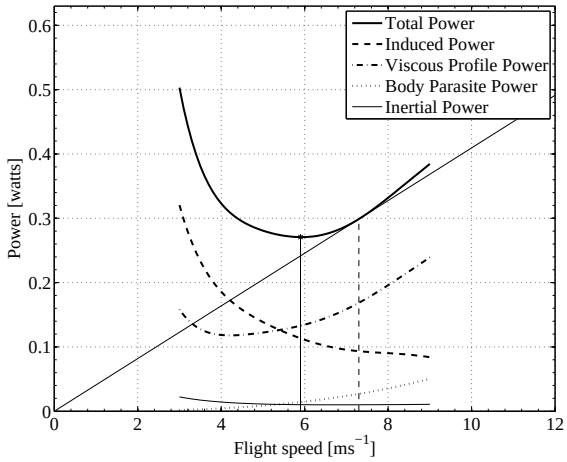

Figure 1: The bat total power, viscous power, induced power, and inertial power components as predicted using the wake-only energetics model [4, 5]

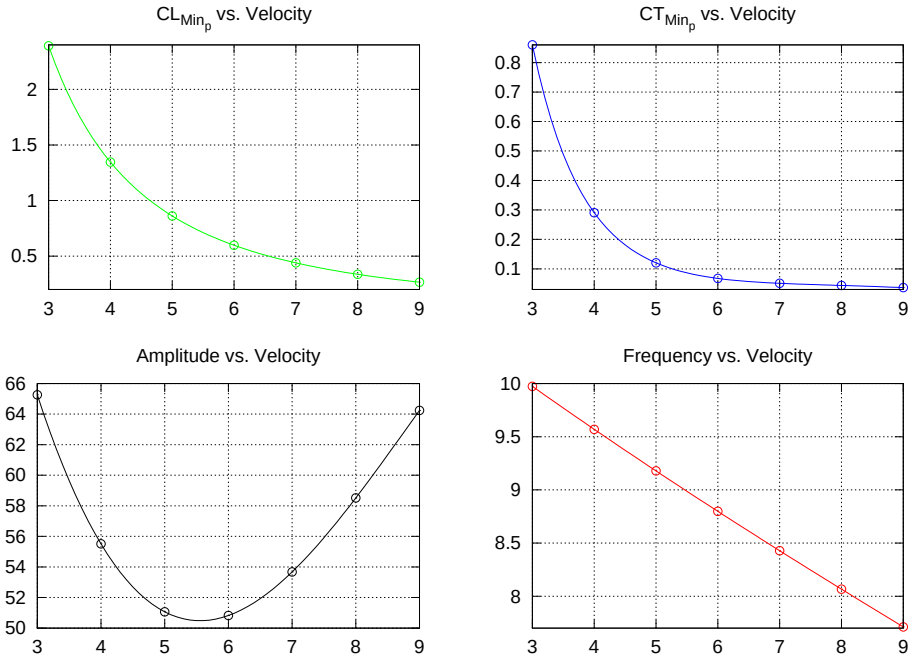

Figure 2: The lift, thrust, amplitude and frequency variations with velocity computed using the wake-only energetics model [4, 5]

Overall, the energetics model shows good agreement with its predecessors as well as with experimental data when considering flight power predictions. In addition to showing good agreement with power predictions, we are also able to predict the flapping amplitude and flapping frequency – with good comparison with experimental observations of flap-

ping. This energetics model is a unique tool that incorporates one of the more complex aerodynamics analyses for energetics evaluation and, to the authors best knowledge, is the first energetics model capable of robustly predicting both the power requirements for flight and the associated best flapping kinematics for a particular wing.

2.2 Using a Collection of Optimal Circulation Wakes for Wing Design

A valuable result that is rarely used in the basic energetics analysis is the predicted optimal wake-circulation distribution. This wake-circulation distribution is a preliminary indication of the best distribution of fluid kinetic energy in the wake for a given flight force requirement. The wake circulation distribution illustrates the fluid dynamics mechanisms of force production independent of the geometry that produced the forces – essentially forming a fluid dynamic analogy of a terrestrial footprint. This is a particularly useful representation when considering the energetics of flight, since it alleviates most of the flapping wing geometric parameters. however, when it comes to MAV wing design, the end goal is an efficient wing geometry. As such, we illustrate a novel approach for developing a geometry from the wake only circulation distribution.

2.2.1 The Optimal Circulation Wake

The predicted optimal wake-circulation distributions are shown in figure 3 for an exemplar flapping wing animal, the *Cynopterus brachyotis*. These wake-circulation distributions are for a much simpler flapping motions (simple harmonic flapping), than those which would actually be observed in nature. From the standpoint of micro aerial vehicle design, it is preferable to maintain a simple flapping mechanism. Hence, the goal is to achieve similar aerodynamics capabilities as bats or other fliers, while minimizing the complexity of the flapping motions.

2.2.2 Theory: Optimal Circulation Wakes for Wing Design

In this section we describe how the optimal circulation wakes are used for inverse wing-shape design. To determine the MAV wing shape while flying, we use the wake shape and the wake-circulation distribution as the constraints in a boundary element, doublet lattice method. The wake-only result defines the energetics and momentum footprint of the flier on the fluid in the region trailing the wing. Prior to this paper, we briefly described a method that works well for large aspect ratio wings [1], and we propose here an improved inverse design process that is based on directly morphing the wing geometry int he doublet lattice method to directly match the target wake-circulation distribution.

The key result of the wake-only energetics analysis used here is the spatial circulation distribution which is represented using a vortex/doublet lattice. This discrete spatial circulation distribution and the forward velocity of the flapper combine to give a discrete representation of timesteps in the flapping cycle. The wake-circulation distribution be-

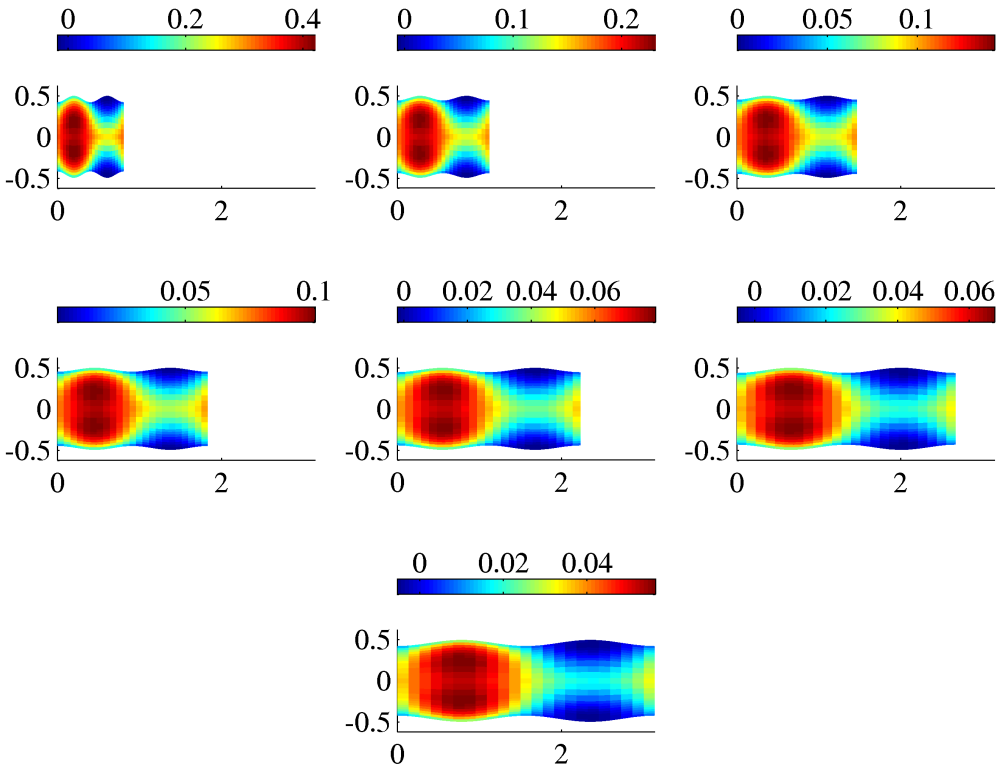

Figure 3: The combined *HallOpt* and energetics model predicted optimal circulation distribution in the wake behind a MAV inspired by a *Cynopterus brachyotis* [4, 5]. Here the wake is represented in nondimensional dorm, ie. $\hat{b} = 1.0 = \frac{b}{b}, \hat{U} = 1.0 = \frac{U}{U_\infty}, \hat{\Gamma} = \frac{\Gamma}{U \cdot b^2}, etc.$. This nondimensional representation allows us to simply design a nondimensional wing and then scale by the appropriate dimensionalization.

comes the target or goal circulation distribution for the flapping wing. Having chosen a wing planform *a-priori* the morphed wing shape (by some combination of incidence angle adjustments or camber adjustments at different spanwise locations) at each successive timestep is the desired outcome. This can be determined in the following two approaches:

1. **Initial large aspect ratio method**: The first method proposed [1] required finding the wing shape corresponding to a feathered or zero-force configuration. Once this feathered shape was determined, the desired wing incidence to produce the flight forces was subsequently superimposed using a steady quasi-lifting-line approach. This shape was then evaluated in *FastAero* [8], to determine the accuracy of the wake circulation production. This wing design methodology worked adequately for higher aspect ratio wings ($AR > 7$) when a weak iterative process was used. The method typically converged to a reasonable wing-shape representation within five

to ten iterations. As seen in the description of this method [1] the target wake was only approximately achieved, however, the force production was fully accomplished.

2. **A novel quasi-inverse design method**: The local wing shape can be manipulated by either adjusting the camber and/or the local incidence angle of the wing to achieve the desired circulation distribution in a pseudo-inverse manner. At each timestep of the doublet lattice method the wing incidence or camber at different spanwise locations is an unknown. Using wing geometric variables (here incidence angle), we have developed a method to tune the shape of the wing until the circulation distribution in the wake matches the wake-only target to within a desired tolerance. The resulting wing design process becomes one in which the local wing shape (incidence and camber) is determined at each discrete timestep of the representation using an unsteady doublet-lattice solver. The resulting doublet lattice method differs from traditional implementations in that the end goal is to determine the shape of the wing that produced the desired wake distribution, rather than the more traditional analysis which is to evaluate the effect of the wing on the fluid.

In the section that follows we describe the theory and numerics involved in the present pseudo-inverse wake-only-to-wing-geometry design process.

2.2.3 Theory: Optimal Circulation Wakes for Wing Design

The wake circulation distribution represents the wing momentum transfer influence of the wing on the fluid. As a result of Helmholtz's and Kelvin's vortex laws we know that the spanwise vorticity in the wake is a direct result of the time-dependent change in the wing bound vorticity, while the streamwise vorticity in the wake is proportional to the wing bound circulation of the wing for that particular point in space. This intimate link between the force production on the wing and the circulation in the wake allows us to link the shape of the wing to the wake circulation at that particular location in space (or time).

The wake is represented using a potential flow, thin-doublet-sheet, that produces the required potential jump to generate the desired lift. At each location in the wake, the potential jump, or circulation corresponds to the circulation that was shed from the trailing edge as it passed the particular location in space. Typically in a doublet lattice, potential flow method the shed wake is unknown and is determined using a Kutta condition of choice. In this particular analysis, the current timestep shed wake strength is known (predicted using the wake-only analysis) and the shape of the wing that produced that particular shed circulation is unknown. As such, the problem becomes one in which the wing shape is determined iteratively by successive adjustments of the wing shape-parameters.

In the section that follows, the pseudo-inverse wing design, doublet lattice method is described.

2.2.4 Numerical Implementation: Optimal Circulation Wakes for Wing Design

The MAV flapping wing shape over a flapping cycle is determined from a wake-only representation (wake shape and wake circulation strength) using the following numerical steps:

1. Run the energetics model to determine the wake shape and the optimal circulation distribution for the particular vehicle characteristics.

   (a) Determine the best kinematics (flapping frequency and amplitude) for a range of velocities for a particular vehicle design (weight, wingspan, etc.).

   (b) Following the energetics evaluation, the optimal wake shapes and circulation distributions are computed using a non-dimensional wake-only analysis. This circulation distribution forms the basis for the rest of the wing design.

   (c) The wake circulation distribution corresponding to the desired flight velocity is loaded into the inverse design tool.

2. Define the *planar* wing planform shape *a-priori*. This involves defining the wing planform in a two-dimensional plane (including wing chord at different spanwise locations). In our definition of the wing geometry, separate routines are used to account for the local wing twist (and camber) as well as the flapping motions – this allows us to concentrate on the different features of the quasi-inverse wing design. The wing is initially defined and discretized in a plane (figure 4). We use the following approach to define the wing planform:

   (a) Here, the leading and trailing edge wing shape is determined using a parametrized quadratic; however, many options for describing the leading edge shape are possible.

   (b) The baseline planar wing is discretized using quadrilateral panels. A list of connectivity and vertices is stored.

   (c) A series of spanwise stations are defined for the planar, reference wing at which quantities such as camber and incidence can be easily modified. These spanwise stations permit wing morphing at different locations along the span.

3. Morph or transform the reference *planar* wing into the actual flying wing geometry (The pseudo code described above is the basis for the current wake-only pseudo-inverse design methodology. While the implementation is significantly involved, the basic principle surrounding the quasi-inverse doublet lattice wing design is straight-forward.

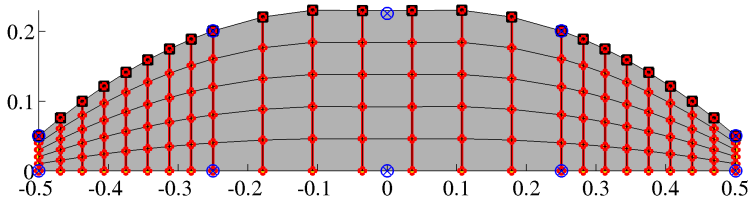

Figure 4: The wing planform for the example used in this paper. The blue dots indicate the $x-$ and $y-$ locations of the leading and trailing edge quadratic fit points (for the leading edge, $(x_1, y_1) = (0.225, 0.00)$, $(x_2, y_2) = (0.200, 0.25)$, $(x_3, y_3) = (0.050, 0.50)$, and for the trailing edge, $(x_1, y_1) = (0.000, 0.00)$, $(x_2, y_2) = (0.00, 0.25)$, $(x_3, y_3) = (0.00, 0.50)$) . The black squares on the leading edge indicate the rotation point about which the incidence angle is measured. The red chordlines indicate the spanwise stations at which the incidence can be changed.

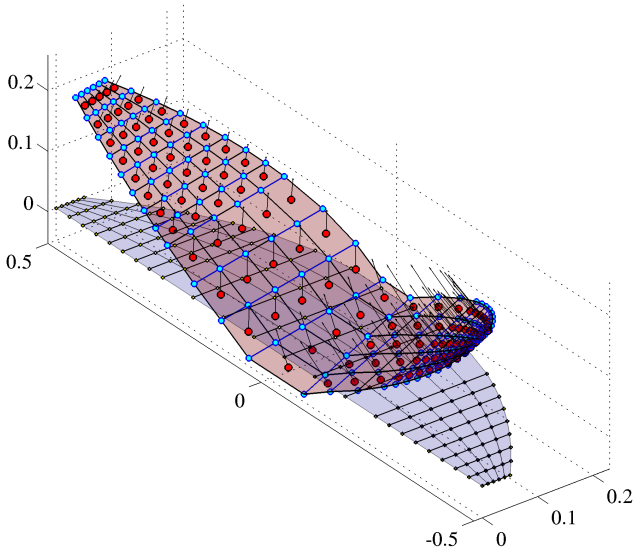

Figure 5: The wing planform is converted into the actual wing shape at each timestep and each sub-iteration of the wing geometry finding routine. First the wing incidence is applied to the individual stations along the span of the wing, and then the entire wing semi-span is transformed to the location corresponding to the kinematics parameters predicted in the wake only method. Here the planform wing is shown as a shadow below the actual flying wing (shown in transparent red). The actual flying wing has a series of quadrilateral panels that are defined using the transformed vertex list (vertices are the blue dots) and a connectivity list. The panel centroids (red dots) as well as the normals are shown in this figure.

3 RESULTS AND DISCUSSION

The results for a *Cynopterus brachyotis* inspired fictional MAV flapping wing design are examined. Although a full range of velocities could be examined, we simply chose four

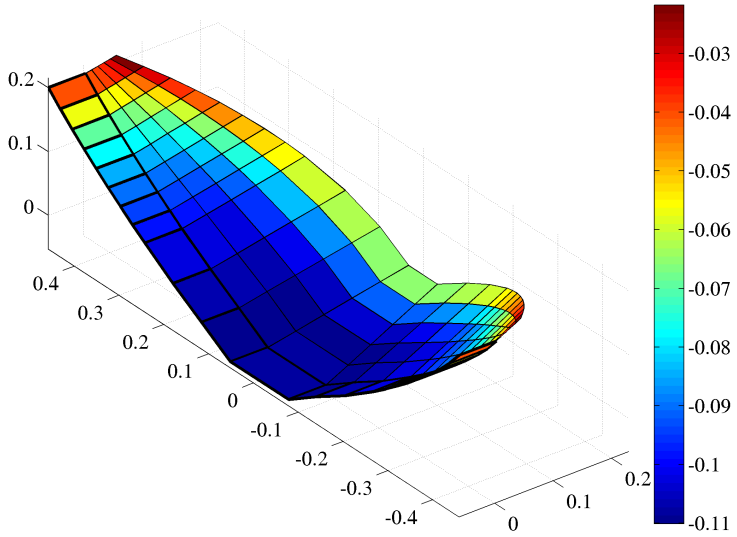

Figure 6: Once the actual flying wing shape is known, a doublet lattice potential flow solution is performed to assess the circulation shed into the wake during that timestep. If the circulation is sufficiently close to the target shed circulation, the wing shape is determined. If the shed circulation does not fall within the desired tolerance, further iteration of th wing shape is necessary. Here the doublet potential strength distribution is shown over the wing and the first timestep of the wake. The first timestep of the wake (the buffer wake) is shown with bold lines.

representative velocities for the current paper, $5m/s, 6m/s, 7m/s$ and $9m/s$ (see Figures 7- 10 respectively).

The different results of the wing design are illustrated in each of the collection of figures (figures 7-10). Of particular interest in the figures is the good agreement between the achieved wake circulation distribution (middle-left) and the target wake distribution (middle-right) (in both of these plots the vehicle is flying from left to right). This agreement between the target and the achieved wake circulations shows that it is feasible to design a reasonable wing shapes with higher theoretical performance than many current MAV designs. Furthermore, this analysis lends some deeper understanding of bio-inspired flight. The ability to tune the wing shape at each spanwise location while simultaneously solving the potential flow, three-dimensional aerodynamics allows us to almost perfectly match the desired wake circulation distribution and wake shape by simply adjusting the local incidences.

The results also show the wing shape morphing during the flapping cycle (top-left image). This wing (flying from right to left in this series of images) shows the zero-force or feathered configuration (in black lines) and the force producing configuration in red lines. It is interesting to note that at lower velocities the difference between the feathered wing condition and the force producing condition is substantial; however, at

faster speeds the two geometries are much closer. This is a direct consequence of the increased dynamic pressure that results from faster flight speeds. From this we can see that the induced aerodynamics components are less critical at higher speeds as expected from earlier energetics predictions. In addition, we can postulate that the design of passively compliant (or mostly passive) flapping wings, although challenging, can be achieved.

In addition to the actual geometry, we also present the wing incidence calculations (bottom row of images in each figure series – again the vehicle is flying from left to right in all images in this sequence). The fist image in that sequence (bottom-left) is the wing incidence angle for the zero-force or feathered wing. As expected, this incidence angle is symmetric and scales with the path of the wing; therefore, as flight velocity increases, the feathered wing requires less local morphing to accomplish the zero-force state. The feathered or zero-force state is a particularly interesting configuration since it represents the simplest possible wing design. In addition, it is simple to postulate the required leading edge torsional resistance that would be required to generate flight forces.

The second image in the incidence angle sequence (bottom-center) illustrates the absolute incidence angle of the local sections of this wing as a function of time (or space). We note several interesting features here. First, the wing requires a more aggressive incidence angle during the downstroke in order to generate the majority of the forces during this period of the flapping stroke. While expected, the current wing design methodology provides insight into the magnitude of the angle during the downstroke vs. upstroke for the particular geometry being examined. We also observe that the wing geometry has a significant impact on the local incidence or angle of attack. We see this at the tips of the flapping wing where the chord is significantly smaller. Due to the decreased chord, the wing must produce lift using a smaller effective area; hence, it must more aggressively angle the wing to the flow at the outboard sections. In addition, we notice that the center of the wing has a near average angle of attack at each different flight velocity. We equate this mean wing-centerline incidence to the body pitch of the flight vehicle. As the flight velocity decreases, this body pitch angle increases. This rather predictable result is also observed in nature [12] and will be the focus of a future investigation.

The third image (bottom-right) in the incidence angle sequence illustrates the wing morphing angle between a zero-force feathered condition and a force producing geometry. This is considered to be an approximation of the local angle of attack at the particular wing section location. This provides us with a preliminary indication of the linearized lift production. The slower velocities (figures 7- 8) demand higher angles of attack than faster flights (figures 9 - 10). This is expected due to the challenge in creating adequate lift to sustain level flight at slower speeds. Also, we can see from the image, the higher angles of attack are demanded in the regions of the wing far away from the vehicle centerline. This is primarily due to the fact that a smaller chord section is being used to generate significant forces. These extreme forces on the outer portions of the wing suggest a strong likelihood of flow separation. While a traditional separation avoidance strategy might suggest a larger chord at the wing-tips, the indication from nature's fliers is that a lower

chord is a feasible design feature. As such, we postulate that this aggressive wing-tip shape may be the cause for stable leading edge vortex effects in smaller, lower Reynold's number fliers. This is an ideal future test case for full fidelity physics simulations (Navier-Stokes).

This methodology has the potential to permit rapid design and analysis of the flapping wing parameter space. Furthermore, a preliminary understanding of the basic considerations in flapping wing design can be achieved. The method naturally handles camber variations across the span of the wing, which may become a useful feature when force and moment constraints are applied for wing design. In addition, adaptive camber may provide a means to align the leading edge of the membrane wing with the flow to reduce the likelihood of separation. Furthermore, with camber and angle of attack as degrees of spanwise freedom, we may be able to effectively design wing structures to allow mostly passive wing morphing. We will examine these modifications and advancements in a future research study.

4 CONCLUSIONS

In this paper we have described a new approach for using low fidelity wake-only energetics results in the inverse design of flapping wings. The process requires some modification of a traditional doublet lattice method and results in a robust method for determining the time dependent morphing of the flapping wing. The method can be used with both camber and/or incidence angle changes, although here only incidence angle changes were examined.

5 Acknowledgements

The authors are grateful for the support from the Air Force Office of Scientific Research (AFOSR) MURI on biologically inspired flight as well as the College of Engineering at the University of Massachusetts Lowell Faculty Startup for the funding of this research.

REFERENCES

[1] D.J.Willis, E.R.Israeli, P.O.Persson, M.Drela, J.Peraire, S.M.Swartz and K.S.Breuer, *A computational framework for fluid structure interaction in biologically inspired flapping flight*, presented at AIAA Conference, AIAA-2007-3803, Miami, FL, June 2007.

[2] D.J.Willis, E.R.Israeli, and J.Peraire, *COMPUTATIONAL INVESTIGATION AND DESIGN OF COMPLIANT WINGS FOR BIOLOGICALLY INSPIRED FLIGHT VEHICLES*, Presented at the 25th ICAS, Anchorage, Alaska, Sept. 2008

[3] Hall, K. C., Pigott, S. A., and Hall,S. R.,*Power Requirements for Large-Amplitude Flapping Flight*, Journal of Aircraft, Vol. 35, No.3, 1998, pp. 352-361

[4] H. Salehipour and D. J. Willis, [**?**], Presented at the 2010 Aerospace Sciences Meeting and Exhibit, Orlando, FL, 2010

[5] H. Salehipour and D. J. Willis, *A NOVEL ENERGETICS MODEL FOR EXAMINING FLAPPING FLIGHT IN NATURE AND ENGINEERING*, To be presented at the 2010 ECCOMAS, 5th CFD Conference, Lisbon, Portugal, 2010.

[6] D.J. Willis, P.O.Persson, E.R.Israeli, K.S.Breuer, S.M.Swartz, J. Peraire, *Multifidelity Approaches for the Computational Analysis and Design of Effective Flapping Wing Vehicles*, Invited Paper, Proceedings of the 46th AIAA Aerospace Sciences Meeting and Exhibit, Reno, Nevada, January 2008.

[7] D.J.Willis, J.Peraire, M.Drela, and J.K.White, A numerical exploration of parameter dependence in power optimal flapping flight, presented at AIAA Conference, AIAA 2006-2994, San Francisco CA, June 2006

[8] D.J.Willis, J.Peraire and J.K.White, A Combined pFFT-multipole tree code, unsteady panel method with vortex particle wakes, Int. J. Numer. Meth. Fluids, 53, 1399-1422, 2007

[9] M. Drela, "Integrated Simulation Model for Preliminary Aerodynamic, Structural, and Control-Law Design of Aircraft." Paper AIAA 99-1394, 40th AIAA SDM Conference, April 1215, 1999 St.Louis, MO.

[10] J. Peraire and P.-O. Persson, *A Compact Discontinous Galerkin (CDG) method for Elliptic Problems*, SIAM J. Sci. Comput., Vol. 30, No. 4, pp. 1806-1824, 2008.

[11] P.O.Persson, D.J.Willis, J.Peraire, *The Numerical Simulation of Flapping Wings at Low Reynolds Numbers*, Presented at the 2010 Aerospace Sciences Meeting and Exhibit, AIAA 2010-724, Orlando, FL, 2010.

[12] Riskin, D.K., Willis, D.J., Diaz, J.-I., Hedrick, T.L., Kostandov, M., Chen, J., Laidlaw, D.H., Breuer K.S., and Swartz, S.M., *Proper Orthogonal Decomposition as a Tool for Analyzing the Complex Kinematics of Bat Flight*, J. Theoret. Biol. 254, 604-615, 2008.

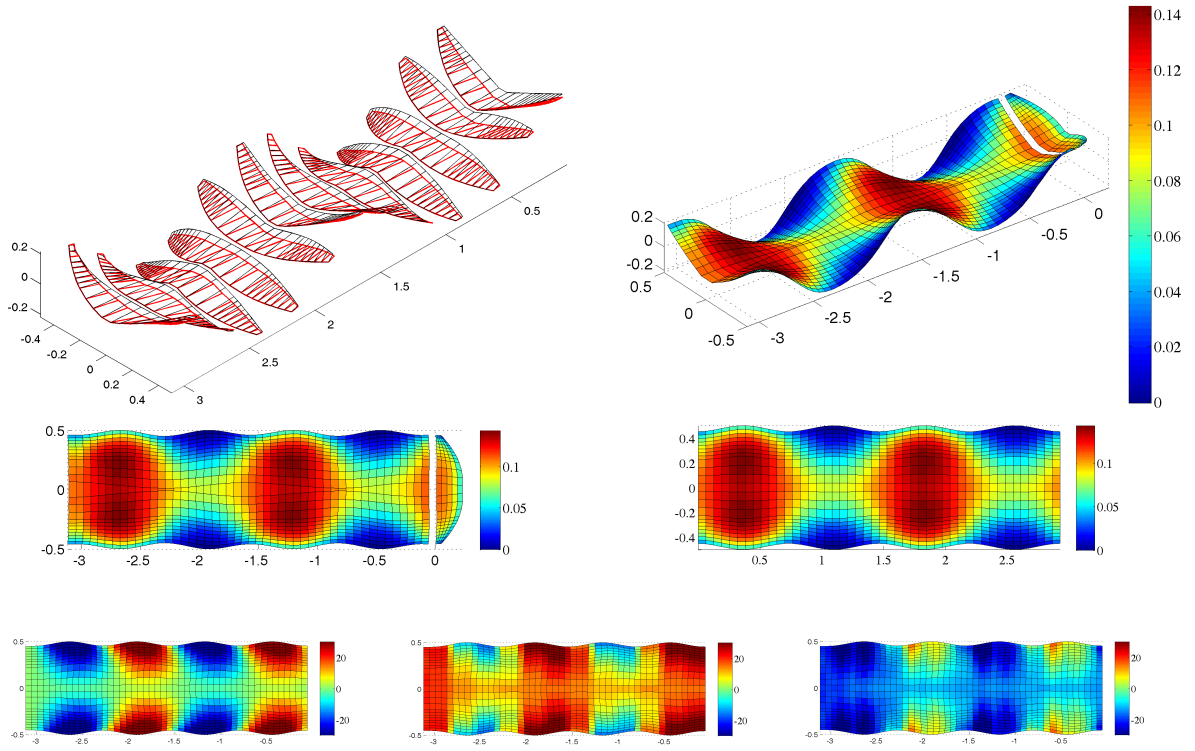

Figure 7: Results for the $5m/s$ wing design case. (Top-left) The three dimensional wing design showing the feathered wing (black lines) and the optimal force producing wing (red-lines). (Top-right) The three dimensional wake and wing solution after two cycles of flapping. (Middle-left) The wake due to the designed win. (Middle-right) The target wake geometry and circulation strength. (Bottom-left) A spatial representation of the local incidence as a function of the flapping cycle position for a zero-force producing, feathered wing. (Bottom-center) The spatial representation of the local incidence as a function of the flapping cycle position for a force producing, optimally designed wing. (Bottom right) The evolution of the wing local angle-of-attack (difference between feathered wing incidence and designed wing incidence).

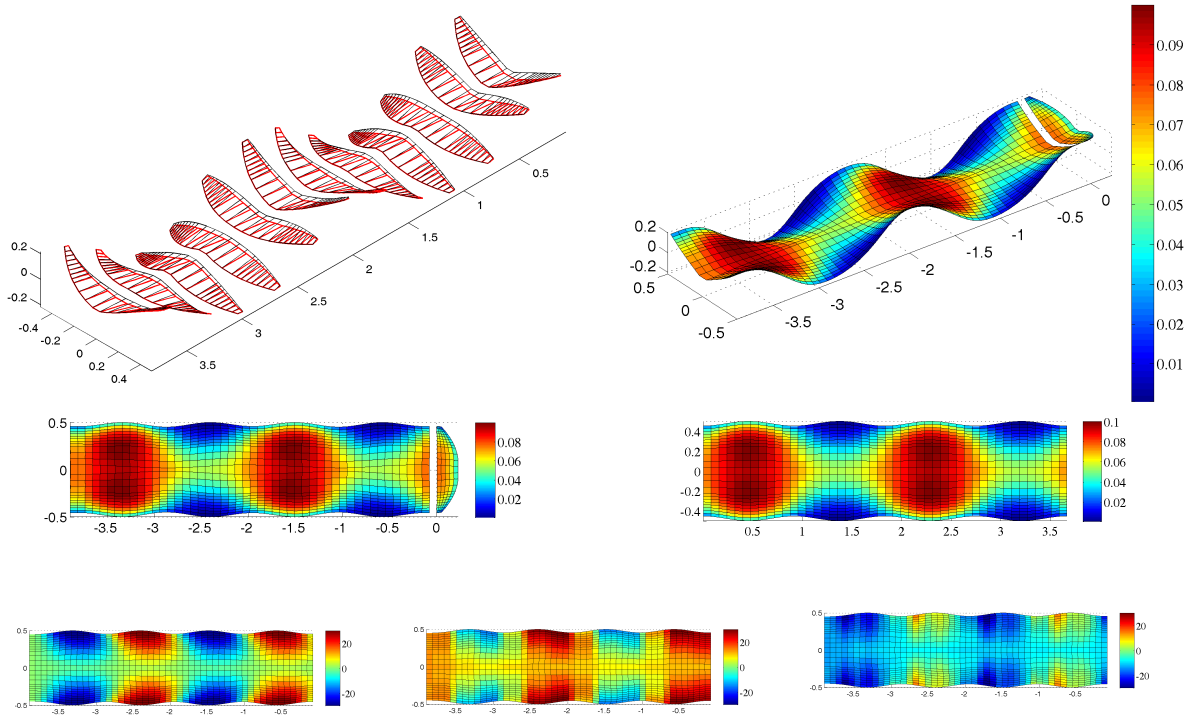

Figure 8: Results for the $6m/s$ wing design case. (Top-left) The three dimensional wing design showing the feathered wing (black lines) and the optimal force producing wing (red-lines). (Top-right) The three dimensional wake and wing solution after two cycles of flapping. (Middle-left) The wake due to the designed win. (Middle-right) The target wake geometry and circulation strength. (Bottom-left) A spatial representation of the local incidence as a function of the flapping cycle position for a zero-force producing, feathered wing. (Bottom-center) The spatial representation of the local incidence as a function of the flapping cycle position for a force producing, optimally designed wing. (Bottom right) The evolution of the wing local angle-of-attack (difference between feathered wing incidence and designed wing incidence).

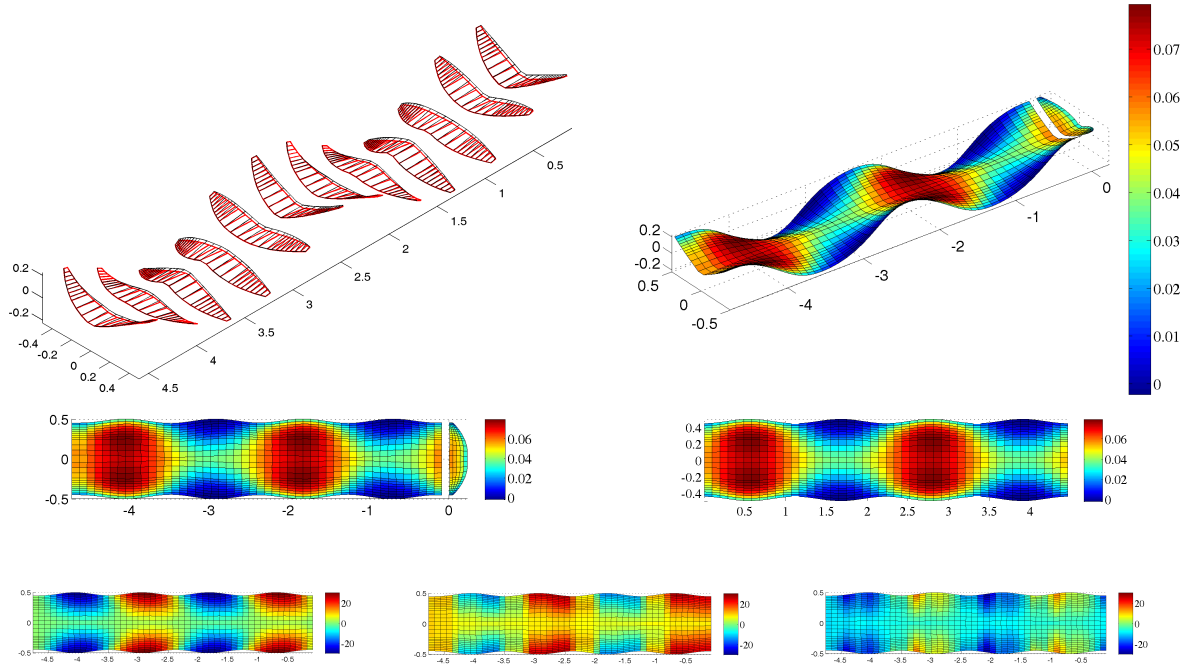

Figure 9: Results for the $7m/s$ wing design case. (Top-left) The three dimensional wing design showing the feathered wing (black lines) and the optimal force producing wing (red-lines). (Top-right) The three dimensional wake and wing solution after two cycles of flapping. (Middle-left) The wake due to the designed win. (Middle-right) The target wake geometry and circulation strength. (Bottom-left) A spatial representation of the local incidence as a function of the flapping cycle position for a zero-force producing, feathered wing. (Bottom-center) The spatial representation of the local incidence as a function of the flapping cycle position for a force producing, optimally designed wing. (Bottom right) The evolution of the wing local angle-of-attack (difference between feathered wing incidence and designed wing incidence).

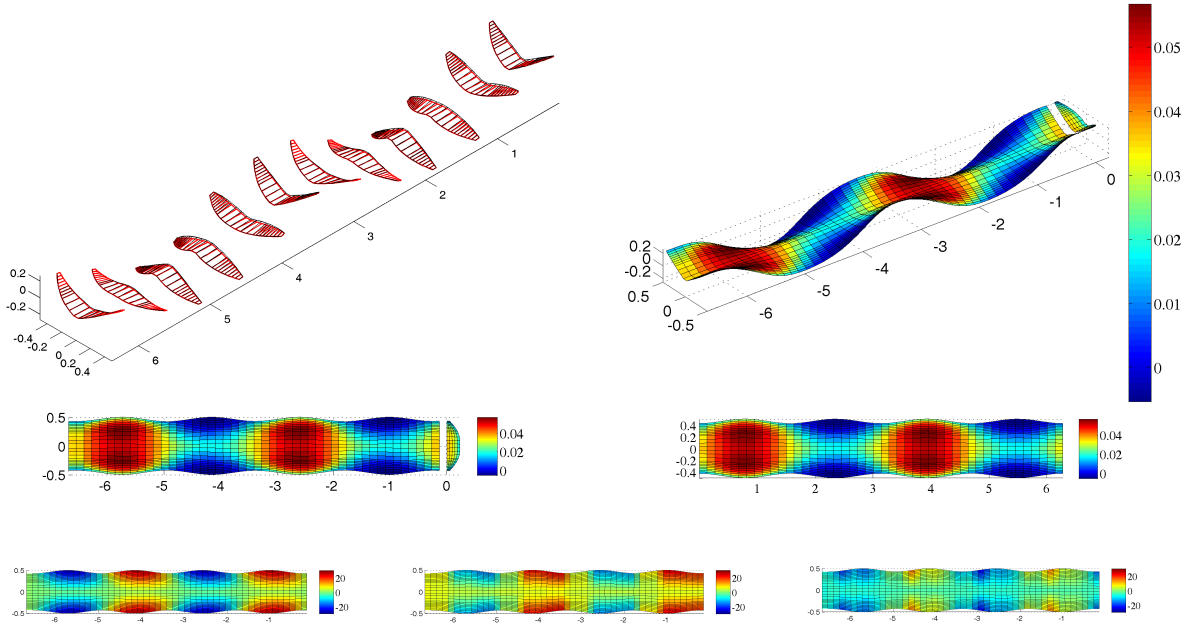

Figure 10: Results for the $9m/s$ wing design case. (Top-left) The three dimensional wing design showing the feathered wing (black lines) and the optimal force producing wing (red-lines). (Top-right) The three dimensional wake and wing solution after two cycles of flapping. (Middle-left) The wake due to the designed win. (Middle-right) The target wake geometry and circulation strength. (Bottom-left) A spatial representation of the local incidence as a function of the flapping cycle position for a zero-force producing, feathered wing. (Bottom-center) The spatial representation of the local incidence as a function of the flapping cycle position for a force producing, optimally designed wing. (Bottom right) The evolution of the wing local angle-of-attack (difference between feathered wing incidence and designed wing incidence).